

## A Helium Cryostat with Pumping of $^3\text{He}$ Vapors for Optical Investigations

A. V. Gorbunov<sup>a</sup>, E. I. Demikhov<sup>a,b,c</sup>, S. I. Dorozhkin<sup>a</sup>, K. P. Meletov<sup>a,b</sup>, and V. B. Timofeev<sup>a</sup>

<sup>a</sup> Institute of Solid State Physics, Russian Academy of Sciences,

ul. Institutskaya 2, Chernogolovka, Moscow oblast, 142432 Russia

<sup>b</sup> OOO RTI, Cryomagnetic Systems, ul. Institutskaya 2, Chernogolovka, Moscow oblast, 142432 Russia

<sup>c</sup> Lebedev Physics Institute, Russian Academy of Sciences, Leninskii pr. 53, Moscow, 119991 Russia

Received June 8, 2009

**Abstract**—The construction of a helium cryostat with pumping of  $^3\text{He}$  vapors designed for optical measurements with a high spatial resolution in the temperature range 0.45–4.20 K. The cryostat is equipped with four windows made from fused silica. A studied sample is mounted inside a reservoir filled with liquid  $^3\text{He}$  in a holder minimizing the influence of both vibrations and thermal drifts and can stay in the chamber at  $T = 0.45$  K for  $>20$  h. The cryostat was used to study photoluminescence of GaAs/AlGaAs semiconductor heterostructures. It was revealed that, in a structure with two tunnel-coupled GaAs quantum wells with a width of 120 Å, the threshold pumping power required for the appearance of a narrow spectral line, which corresponds to the Bose condensate of spatially indirect dipolar excitons, decreases by a factor of 6, as the temperature falls from 1.50 to 0.45 K. In a sample with a single wide (250 Å) GaAs quantum well, the distribution patterns of the luminescence of dipolar excitons inside a 5- $\mu\text{m}$  circular potential trap were obtained at  $T = 0.45$  K. The spatial resolution of the distributions is no worse than 1.5  $\mu\text{m}$ .

PACS numbers: 07.20.Mc, 71.35.Lk, 78.67.De

DOI: 10.1134/S0020441209060256

In the field of optical spectroscopy of condensed media, there exist a number of interesting problems that can be solved at  $T < 1$  K and a rather high spatial resolution. One of them is associated with investigations of the Bose–Einstein condensation (BEC) of hydrogen-like excitons in semiconductors [1–7]—in particular, with studies of the phase diagram of a transition into a Bose-condensed state at  $T < 1$  K. To solve such a problem, an optical cryostat with pumping of  $^3\text{He}$  vapors is necessary, which would made it possible to perform measurements with a high-aperture optical system ensuring a spatial resolution at a level of 1  $\mu\text{m}$ . In this paper, the design of an optical cryostat we manufactured is described. This instrument allows cooling of samples to  $T = 0.45$  K and conducting of optical studies of BEC of spatially indirect dipolar excitons in GaAs/AlGaAs quantum wells.

### DESIGN OF THE CRYOSTAT

The design of the developed optical cryostat is schematically shown in Fig. 1. In contrast to other designs, here, the studied sample is placed just inside the chamber filled with liquid  $^3\text{He}$  and not in a glass ampoule connected to the  $^3\text{He}$  chamber through a cold finger [8]. This ensures effective cooling of the studied sample to  $0.45 \pm 0.05$  K during pumping of helium vapors and maintenance of this temperature under illumination of the sample with visible light.

The rectangular structure of the cryostat's tail part (see the inset in Fig. 1) allows the distance from the surface of the studied sample to the cryostat's outer window to be reduced to  $<30$  mm, thus making it possible to use an optical system with fast lenses ensuring a spatial resolution of up to  $\sim 1$   $\mu\text{m}$ . The cryostat has the following main characteristics:

Diameter of the column for samples	24 mm
Volume of the vessel for liquid $^4\text{He}$	5 l
Volume of the vessel for liquid nitrogen	4 l
Number of windows	4
Material of windows	KY quartz
Sample–window aperture	33°
Height of windows relative to the low edge of the cryostat	120 mm
Working distance (sample–outer window)	30 mm
Diameter of the outer window	28 mm
Diameter of the inner window	10 mm
Light depolarization	$<1\%$
Volume of the external vessel for $^3\text{He}$	27 l
Minimum temperature of a sample	0.45 K
Time of continuous operation at 0.45 K	$>20$ h
Consumption of liquid helium at 4.2 K	$<0.1$ l/h

Consumption of helium for cooling the cryostat to 4.2 K from the temperature of liquid nitrogen	1.6 l
Length of the tail part	286 mm
Outer dimensions of the tail part	65 × 55 mm
Outer diameter of the cryostat	215 mm
Cryostat height	1285 mm
Cryostat mass	12 kg

To reduce the power of thermal radiation penetrating into the chamber with  $^3\text{He}$  from warm parts of the cryostat, the chamber is surrounded by two copper shields, one of which—outer shield 10—is cooled with liquid nitrogen and the second—shield 12 directly surrounding the chamber with  $^3\text{He}$ —is cooled with liquid  $^4\text{He}$ . To perform optical measurements, each shield has an optical window being in thermal contact with it. As a result, four windows, mounted in the outer shell of the cryostat, nitrogen shield, helium ( $^4\text{He}$ ) shield, and wall of the chamber with liquid  $^3\text{He}$ , are positioned on the optical axis (Fig. 1). The resulting aperture of the cryostat's optical channel is  $33^\circ$ , and the distance from the outer window to the sample in the  $^3\text{He}$  chamber is  $<30$  mm. The round windows are manufactured from KY fused quartz, which is transparent in the UV, visible, and near-IR spectral regions. The thickness of the shields' windows is 1.5 mm, and the thicknesses of the window of the  $^3\text{He}$  chamber and the outer window are 2 and 3 mm, respectively. The windows of the outer shell, nitrogen shield, helium shield, and  $^3\text{He}$  chamber have diameters of 28, 25, 20, and 10 mm, respectively. The outer and  $^3\text{He}$  chamber's windows are hermetically glued into stainless-steel collars with a thickness of  $<150$   $\mu\text{m}$ , which are soldered to the outer shell and the chamber with liquid  $^3\text{He}$ , respectively. A domestic Kri-sil multicomponent epoxy adhesive used for this purpose ensures tightness of joints at low temperatures and high reliability under multiple thermocycling ( $\geq 1000$  cycles). A finely dispersed powder guaranteeing the required mechanical and thermal properties of the adhesive seam is one of the components of this glue. Thin-wall collars allow minimization of elastic strains arising during cooling of windows and substantially reduce their polarizing effect. The БФ-2 glue is used to paste windows to the nitrogen and helium shields. The windows efficiently absorb thermal radiation and withdraw it to the cooled shields. This allows one to significantly reduce the heat supply to the chamber with liquid  $^3\text{He}$ , thereby allowing maintenance of the chamber temperature at a level of  $\sim 0.45$  K for 20 h after condensation of 25 l of gaseous  $^3\text{He}$  (under normal conditions) and pumping of its vapors.

The temperature in the chamber with  $^3\text{He}$  was measured with a ruthenium thermometer. An  $\text{RuO}_2$  resistor was calibrated in the range 1.5–20.0 K using both a calibrated germanium resistor and the pressure

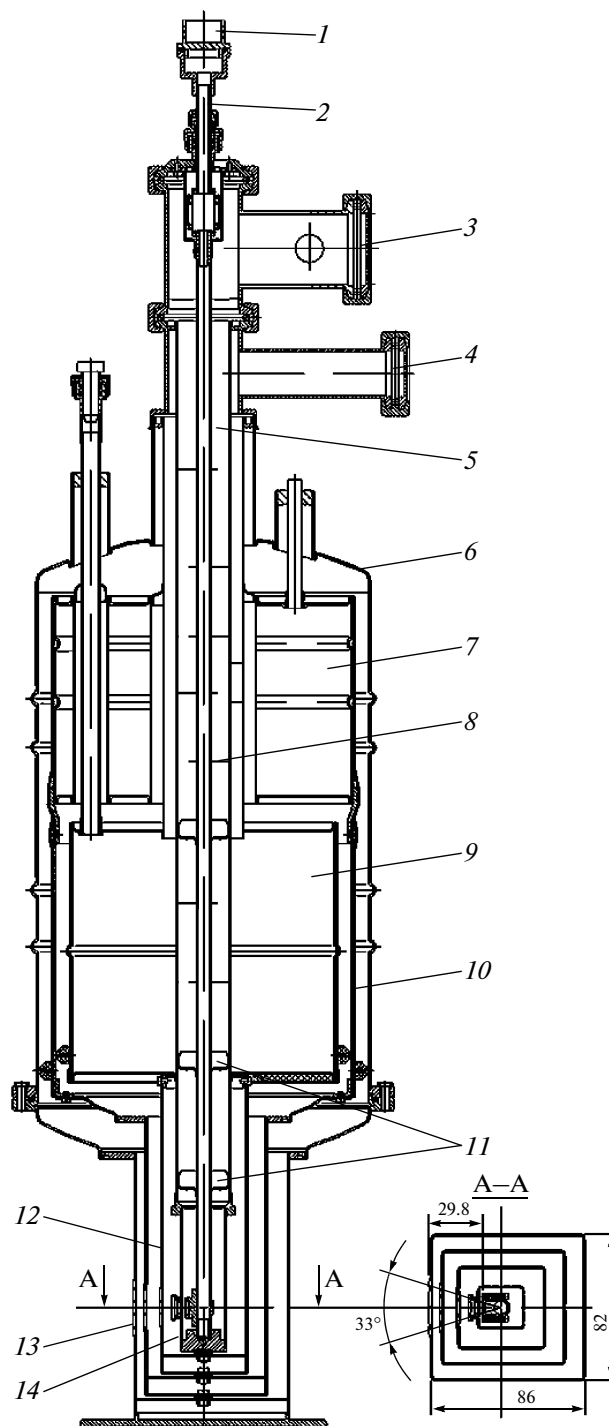


**Fig. 1.** Schematic diagram of the optical cryostat with pumping of  $^3\text{He}$  vapors: (1) electric connector, (2) sample holder, (3) vacuum joint for pumping of  $^3\text{He}$  vapors, (4) vacuum joint for pumping of  $^4\text{He}$  vapors, (5) cylinder, (6) outer shell, (7) vessel for liquid nitrogen, (8) radiation shield, (9) vessel for liquid  $^4\text{He}$ , (10) nitrogen shield, (11) plate-radiators, (12) helium shield, (13) outer optical window, and (14) chamber for samples. The inset shows the cross section of the cryostat's tail.

of  $^4\text{He}$  vapors. In the range 0.45–2.00 K, the thermometer was calibrated by the  $^3\text{He}$  vapor pressure. In all ranges, the calibration accuracy was no worse than 0.05 K. During operation with external continuous photoexcitation sources, in particular, with semiconductor lasers with wavelengths of 659 and 782 nm, when the integral power of the light flux incident on a sample increased to 100  $\mu\text{W}$ , the temperature of the  $^3\text{He}$  chamber increased by a value  $<0.05$  K.

To achieve a high spatial resolution, it is necessary to minimize both mechanical vibrations and relatively slow drifts of a sample caused by temperature variations in the upper part of the cryostat. To prevent sample vibrations, the lower conic part of sample holder 2 was pressed against a conical notch in the bottom of chamber 14. A bellows element positioned in the upper part of the sample holder's rod served as a spring. The position of the holder inside cylinder 5 was fixed by elastic spacers relative to the walls of the cylinder, which is a line for pumping of  $^3\text{He}$  vapors rigidly joined to the rectangular  $^3\text{He}$  chamber. This reduced rod vibrations in the direction perpendicular to the cryostat axis.

Let us discuss the cryostat design in more detail. The CRYO105\_He3 helium cryostat (according to the nomenclature of RTI, Cryomagnetic Systems Co.) with pumping of  $^3\text{He}$  vapors was produced on the basis of a modified OptCRYO105 helium optical cryostat [9] and intended for optical investigations in the temperature range 0.45–4.2 K. Thin-wall stainless-steel cylindrical column 5 has dimensions of  $\varnothing 24 \times 0.3$  mm and serves as a route for pumping  $^3\text{He}$  vapors. In its lower part, the cylinder is hermetically joined to rectangular chamber 14 for samples, which is manufactured from copper sheets 0.8 mm thick. Shields 10 and 12 are made of the same material. A sample fixed in the holder is loaded into the chamber through a hole in the upper part of cylinder 5. Outer shell 6 of the cryostat is manufactured from stainless steel sheets 1.2 mm thick. The vacuum volume of this shell contains vessels 7 and 9 for liquid nitrogen and  $^4\text{He}$  with volumes of 4 and 5 l, respectively, manufactured from the same stainless steel sheets (Fig. 1). All vacuum seams of the outer shell and the inner vessels of the cryostat were made using argon-arc welding. After being manufactured, all components were electropolished.

The vessel with  $^4\text{He}$  is protected from thermal radiation by copper shield 10 cooled with liquid nitrogen. Vapors are pumped from the  $^4\text{He}$  vessel through demountable vacuum ring joint 4 using an external mechanical pump (Edwards E2M28 with a capacity of 32  $\text{m}^3/\text{h}$ ). As a result of pumping, the temperature of the  $^4\text{He}$  volume decreases to 1.45 K, which is sufficient for the condensation of gaseous  $^3\text{He}$  stored in a receiver at room temperature. Simultaneously, the temperature of copper shield 12 surrounding the  $^3\text{He}$  chamber also decreases. A temperature of 1.45 K is maintained constant during the entire experiment,

and gaseous  $^3\text{He}$  condenses on copper plate—radiators 11 attached to the rod of the sample holder and being in thermal contact with the walls of the  $^4\text{He}$  vessel. Liquid  $^3\text{He}$  is collected on the bottom of the rectangular chamber. After 25 l of gaseous  $^3\text{He}$  condense and are cooled to 0.45 K by pumping of its vapors, the liquid level remains above optical window 13, so that the sample under study is completely immersed in liquid  $^3\text{He}$ .  $^3\text{He}$  vapors are pumped with an external cryosorption pump through demountable vacuum ring joint 3 [10]. The  $^3\text{He}$  temperature is maintained near 0.45 K for at least 20 h. A sample is replaced after the cryostat is completely warmed and the entire  $^3\text{He}$  volume is pumped into the receiver.

## EXPERIMENTAL RESULTS

To illustrate the capabilities of the described cryostat, we present the results of studies of the photoluminescence spectra under the conditions of BEC of indirect (dipolar) excitons in a double quantum well in a GaAs/AlGaAs  $n-i-n$  heterostructure as a function of laser pumping. These measurements were performed at  $T = 0.45$  and 1.50 K. In this heterostructure, the width of each well is 120 Å and the wells are separated by a barrier consisting of four AlAs monolayers. Dipolar excitons appear under the conditions of above-barrier photoexcitation at an electric voltage applied perpendicular to the heterostructure layers. Under such conditions, an electron and a hole in an exciton are spatially separated in the direction of the applied field and excitons themselves acquire a static dipole moment even in the ground state. Because of a significant decrease in the overlap of the electron and hole wave functions in the direction of the applied field, the radiation lifetime of dipolar excitons substantially increases and they become long-living (on the nanosecond time scale). The lifetime of a dipolar exciton exceeds the characteristic relaxation time at phonons by several orders of magnitude. Therefore, the collective interaction phenomena in a system of high-density dipolar excitons occur under quasi-equilibrium conditions and the gas of such excitons can be cooled to rather low temperatures determined by the temperature of the crystal lattice that contains these excitons.

Owing to strong dipole–dipole repulsion, dipolar excitons in the studied structures are not combined into molecules or other more complex structures (e.g., charged exciton structures or trions). Therefore, even at high densities, a gas of dipolar excitons remains “monoatomic” until excitons are destroyed via ionization as a result of a Mott transition. Moreover, at low temperatures, as the concentration of the gas of dipolar excitons increases, it does not condense into a liquid; i.e., in a dense system of dipolar excitons, a phase transition of the first order does not occur for fundamental reasons. At the same time, excitons and, in particular, dipolar excitons, are composite bosons

because their resulting spin is integer-valued. Therefore, when critical densities are reached at sufficiently low temperatures, a BEC phenomenon may be observed in a system of dipolar excitons. In 2D systems, the BEC of excitons may occur only under the conditions of lateral (intraplane) spatial confinement, i.e., in lateral traps. Large-scale fluctuations of a random potential [11, 12] and nonuniform electric [13–17] or deformation [18] fields may serve as traps for dipolar excitons. The appearance of BEC is accompanied by macroscopic filling of the lowest state in a trap (a state with a zero quasi-momentum) with excitons and the appearance of large-scale coherence in the system of interacting excitons [19].

In photoluminescence spectra, the transition of excitons to the condensed state is displayed in the fact that, when the optical pumping intensifies, a narrow line arises in a thresholdlike manner. Its intensity near the threshold increases superlinearly above a background related to localized states [11, 12, 19, 20]. Figure 2 shows the corresponding luminescence spectra measured at 0.45 K and different powers of laser photoexcitation. The inset shows the dependences of the intensity of the dipolar-exciton line (after deduction of the background) on the laser-pumping power at temperatures of 0.45 and 1.54 K. As is seen, the intensity of the narrow line near the threshold increases superlinearly with an increase in the photoexcitation power; this could be expected under the conditions of exciton Bose condensation. A linear dependence of the line intensity on the pumping power is observed only far from the threshold. It is of importance that, when the temperature decreases from 1.50 to 0.45 K, the threshold of appearance of the narrow line corresponding to the Bose condensate (indicated with an arrow in Fig. 2) shifts toward lower optical pumping levels and decreases by a factor of almost 6.

The obtained results demonstrate the possibility of further studies of the phase diagram of the BEC of dipolar excitons [12]. The phase diagram must be plotted in the density–temperature coordinates. In this case, the absolute values of the exciton density will be determined using the measured luminescence signal of the exciton condensate, the known geometry of luminescence radiation collection, and the exciton lifetime in the condensate measured from the luminescence kinetics [21]. According to the measurement results, it should be expected that the critical values of the temperature and exciton density will be interrelated via a power law. The value of the exponent will make it possible to evaluate the form of the confining lateral potential and, probably, the very state of imperfection of the system of interacting dipolar exciton under study.

In conclusion, let us consider one more experimental problem associated with studies of BEC of dipolar excitons, which, in principle, will be presumably solved using the described optical  $^3\text{He}$  cryostat. These are measurements of a large-scale spatial coher-

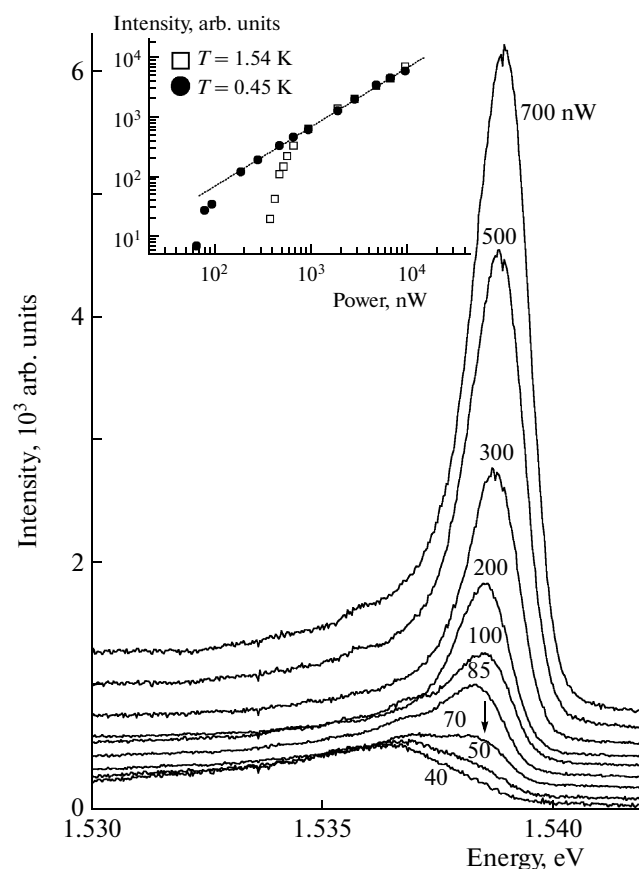


**Fig. 2.** Series of photoluminescence spectra of indirect (dipolar) excitons in a GaAs/AlGaAs double quantum well (the width of both wells is 120 Å) depending on the power of laser ( $\lambda = 659$  nm) pumping (figures near curves) at  $T = 0.45$  K. The inset shows the dependences of the dipolar-exciton line intensity on the pumping power (after deduction of the luminescence background of localized states) at  $T = 0.45$  and 1.54 K. The line onset threshold (the arrow in the spectral series) increases with temperature by a factor of  $\sim 6$ .

ence and the correlation function of luminescence amplitudes  $g^{(1)}$  (first-order correlator) along the BEC phase diagram. Earlier, we showed that, under the condition of Bose condensation, the actual picture of luminescence observed with a high spatial resolution from a circular trap, in which dipolar excitons accumulated, is a spatially periodic structure of luminescing spots [19, 20]. Direct observations of the in situ optical Fourier transform of such a spatially periodic luminescence structure demonstrated its high spatial coherence [19]. However, correlation function of amplitudes  $g^{(1)}(x, y)$  itself as a function of spatial coordinates  $(x, y)$  in the plane of the quantum well and the behavior of the amplitude correlator under temperature variations have not been determined so far. In principle, this problem can be solved using a two-beam interferometer, to which images of a spatially periodic structure of luminescence of dipolar excitons

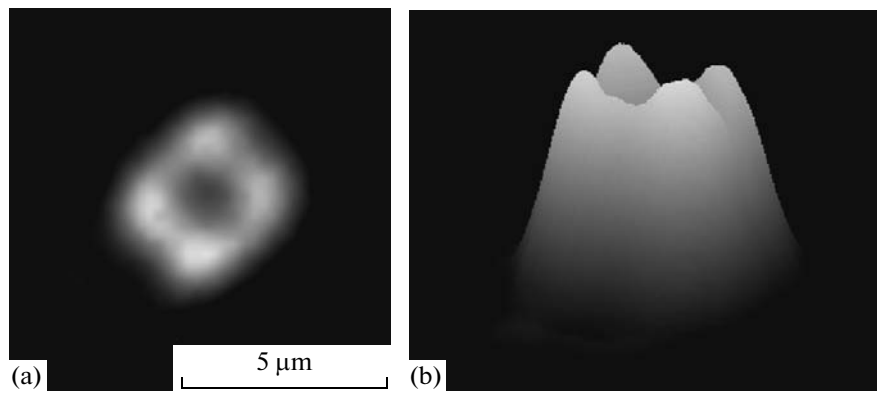


**Fig. 3.** (a) Spatial distribution of the photoluminescence intensity of dipolar excitons inside a 5- $\mu\text{m}$ -diameter circular potential trap and (b) its 3D pseudoimage (the intensity is plotted along the vertical coordinate). A single GaAs/AlGaAs quantum well 250  $\text{\AA}$  wide,  $T = 0.45$  K,  $P = 200$  nW, and  $\lambda = 659$  nm.

from the circular lateral trap are transmitted with a sufficiently high spatial resolution ( $\sim 1$   $\mu\text{m}$ ).

In experiments performed with the described cryostat, we managed to observe in situ spatially periodic structures of luminescence of a Bose condensate of dipolar excitons with a quite high spatial resolution (to  $\sim 1$   $\mu\text{m}$ ). This result (Fig. 3) was obtained at  $T = 0.45$  K. In experiments, a Schottky GaAs/AlGaAs photodiode with a single wide (250  $\text{\AA}$ ) GaAs quantum well was used. Electron-lithography methods were used to form round holes 5  $\mu\text{m}$  in diameter in the Schottky gate. When an electric voltage was applied to the Schottky gate, along the perimeter of such a window, a lateral circular potential well for dipolar spatially indirect excitons arose [19, 20]. Under the conditions of above-barrier photoexcitation, dipolar excitons that were generated in the quantum well accumulated in the circular trap along its perimeter. When the critical pumping and temperature conditions corresponding to the BEC of dipolar excitons are reached, a narrow luminescence line corresponding to the exciton Bose condensate arose in the luminescence spectrum at a certain threshold. At a sufficiently large magnification, the spatially periodical structure of luminescing spots, which also corresponds to the exciton Bose condensate, can be seen in the pattern of luminescence emitted from the trap. To observe a spatially resolved pattern of luminescence directly from the circular trap, we used high-resolution projection optics combined with a narrow-band interference filter, which cut the region of the narrow luminescence line of the exciton Bose condensate in the spectrum. Pseudoimages of the spatially periodical structure indicate that the luminescence spots are resolved with an accuracy no worse than 1.5  $\mu\text{m}$  (Fig. 3). Thus, these images can be transferred with a sufficient resolution to a two-beam interferometer for further measurements and subsequent analysis of the amplitude correlator as a function of spatial coordinates.

### ACKNOWLEDGMENTS

This study was supported by the Russian Foundation for Basic Research of the Russian Academy of Sciences, a program of the Presidium of the Russian Academy of Sciences for Nanostructures and a program of the Branch of the Russian Academy of Sciences for Strongly Correlated Systems.

More detailed information on the cryostat design can be obtained at the website [www.cryo.ru](http://www.cryo.ru) or [ito@issp.ac.ru](mailto:ito@issp.ac.ru).

### REFERENCES

1. *Eksitony* (Excitons), Rashba, E.I. and Sterdzh, M.D., Eds., Moscow: Nauka, 1985.
2. Keldysh, L.V. and Kozlov, A.N., *Zh. Eksp. Teor. Fiz.*, 1968, vol. 54, no. 3, p. 978.
3. Butov, L.V., Lai, C.W., Ivanov, A.L., et al., *Nature*, 2002, vol. 417, no. 6884, p. 47.
4. Snoke, D.W., *Science*, 2002, vol. 298, no. 5597, p. 1368.
5. Timofeev, V.B., Gorbunov, A.V., and Larionov A.V., *J. Phys.: Condens. Matter*, 2007, vol. 19, no. 29, p. 295209.
6. Timofeev, V.B. and Gorbunov A.V., *J. Appl. Phys.*, 2007, vol. 101, no. 8, p. 081708.
7. Timofeev, V.B. and Gorbunov A.V., *Phys. Stat. Sol. C*, 2008, vol. 5, no. 7, p. 2379.
8. Mezhev-Deglin, L.P., Revenko, V.I., and Dite, A.F., *Prib. Tekh. Eksp.*, 1979, no. 6, p. 160.
9. website: [www.cryo.ru](http://www.cryo.ru), OOO "RTI, Cryomagnetic systems."
10. Dorozhkin, S.I., Zverev, V.N., and Merzlyakov, G.V., *Prib. Tekh. Eksp.*, 1996, no. 7, p. 165.
11. Larionov, A.V., Timofeev, V.B., Ni, P.A., et al., *Pis'ma Zh. Eksp. Teor. Fiz.*, 2002, vol. 75, no. 11, p. 689.
12. Dremin, A.A., Larionov, A.V., Timofeev, V.B., et al., *Pis'ma Zh. Eksp. Teor. Fiz.*, 2002, vol. 76, no. 7, p. 526.
13. Gorbunov, A.V. and Timofeev, V.B., *Pis'ma Zh. Eksp. Teor. Fiz.*, 2004, vol. 80, no. 3, p. 210.

14. Hammack, A.T., Gippius, N.A., Yang Sen, et al., *J. Appl. Phys.*, 2006, vol. 99, no. 6, p. 066104.
15. Rapaport, R., Chen, G., Simon, S., et al., *Phys. Rev. B*, vol. 72, no. 7, p. 075428.
16. Chen, G., Rapaport, R., Pfeiffer, L.N., et al., *Phys. Rev. B*, vol. 74, no. 4, p. 045309.
17. Gärtner A., Prechtel, L., Schuh, D., et al., *Phys. Rev. B*, 2007, vol. 76, no. 8, p. 085304.
18. Negoita, V., Snoke, D.W., and Eberl, K., *Phys. Rev. B*, 1999, vol. 60, no. 4, p. 2661.
19. Gorbunov, A.V. and Timofeev, V.B., *Pis'ma Zh. Eksp. Teor. Fiz.*, 2006, vol. 84, no. 6, p. 390.
20. Gorbunov, A.V. and Timofeev, V.B., *Pis'ma Zh. Eksp. Teor. Fiz.*, 2006, vol. 83, no. 4, p. 178.
21. Gorbunov, A.V., Larionov, A.V., and Timofeev, V.B., *Pis'ma Zh. Eksp. Teor. Fiz.*, 2007, vol. 86, no. 1, p. 48.